Supporting information of "The characteristics of submicron particles at a regional receptor site of Central Eastern China: emissions from coal combustion and aging of organic aerosols."

Weiwei Hu[1], Min Hu[1]*, Bin Yuan[1], Jose L. Jimenez[3], Qian Tang[1], Jianfei Peng[1], Wei Hu[1], Min Shao[1], Ming Wang[1], Limin Zeng[1], Yusheng Wu[1], Zhaoheng Gong[12], Xiaofeng Huang[1,2], Lingyan He[1,2]

1 State Key Joint Laboratory of Environmental Simulation and Pollution Control, College of Environmental Sciences and Engineering, Peking University, Beijing 100871

2 Key Laboratory for Urban Habitat Environmental Science and Technology, School of Environment and Energy, Peking University Shenzhen Graduate School, Shenzhen 518055

3 Cooperative Institute for Research in the Environmental Sciences (CIRES) and Department of Chemistry and Biochemistry, Univ. of Colorado, Boulder, CO, USA

1 Location of the obervation site

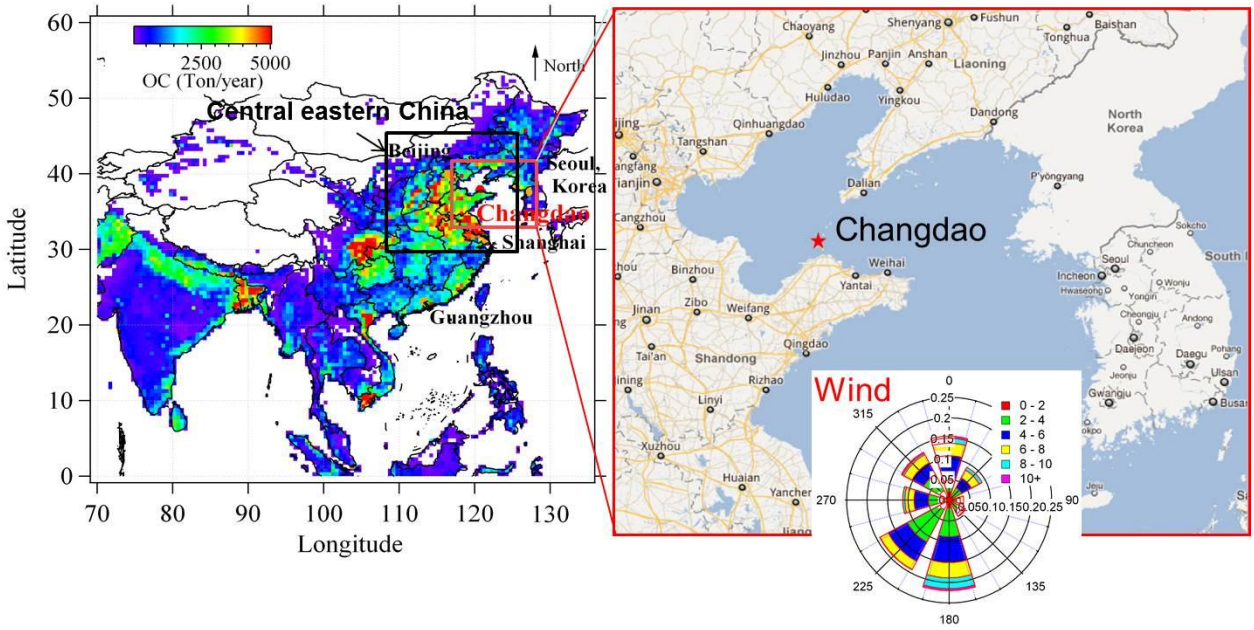

Figure S-1 The location of Changdao site. The boundary of Central Eastern China is shown in the black box. The left panel is color-coded according to the OC emissions (Zhang et al., 2009). The wind rose plot is also shown in the right panel.

2 The predicted NH_4^+ and measured NH_4^+ balance

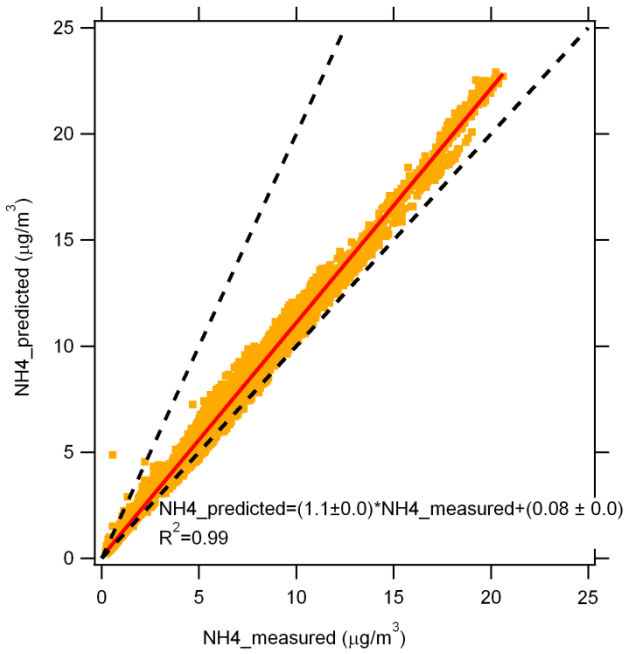

Figure S-2 The predicted NH_4^+ and measured NH_4^+ concentrations at the Changdao site. The predicted NH_4^+ was calculated by assuming full neutralization of particulate anions (NO_3^-, SO_4^{2-}, and Cl^-).

3 Comparisons of aerosol components between AMS and other instruments

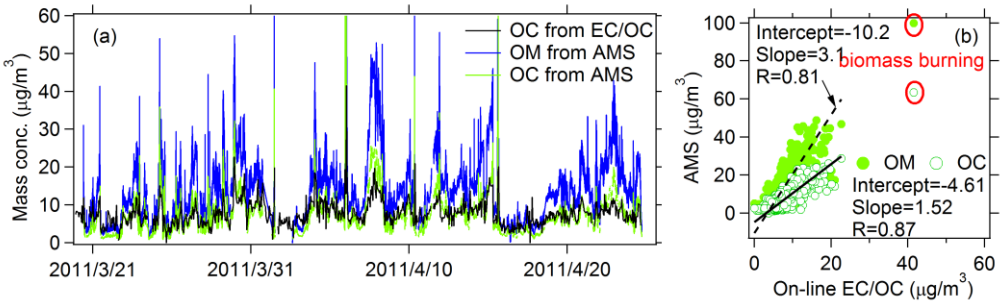

Figure S-3 (a) Time series of OM , OC from AMS and OC from Sunset online EC/OC analyzer; (b) Scatter plots of OM vs. OC and OC from AMS vs. OC from Sunset online EC/OC analyzer. Linear regression results are also shown in the graphs.

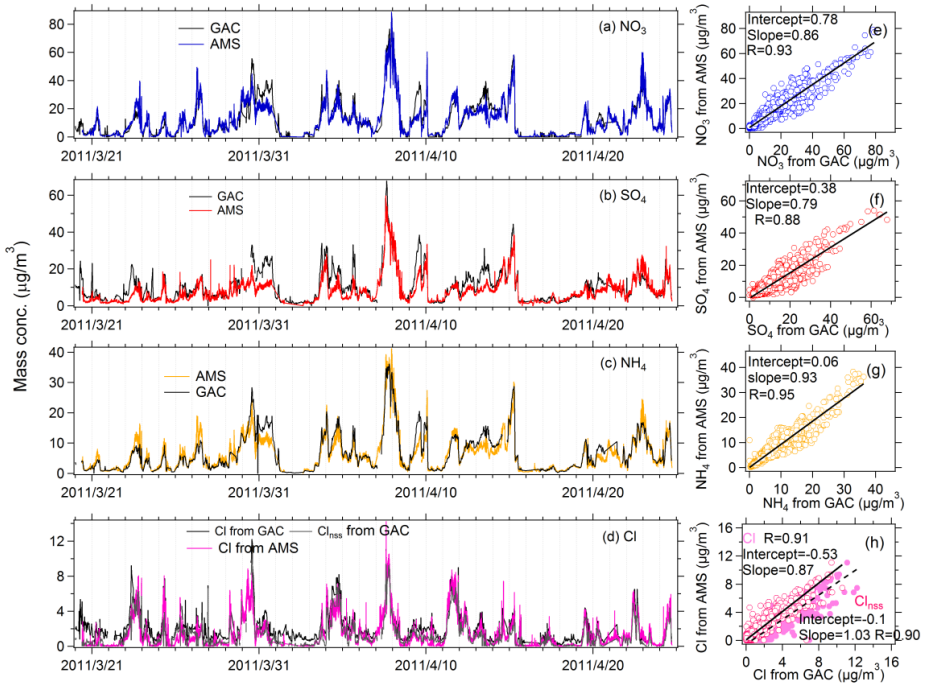

Figure S-4 Inter-comparison of inorganic aerosols between AMS and GAC-IC system.

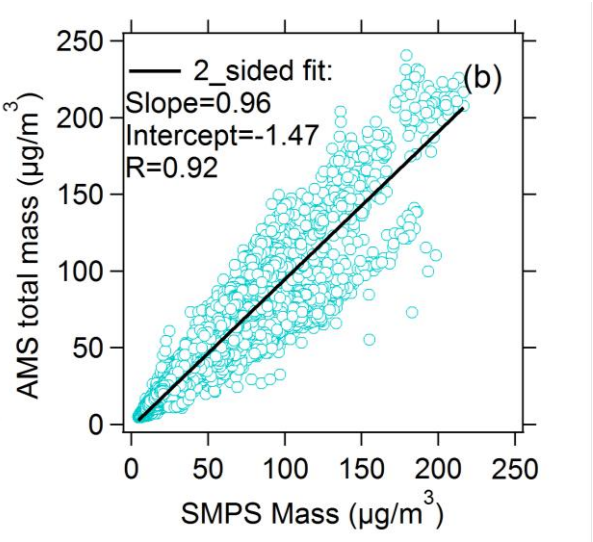

Figure S-5 Scatterplot of NR-PM_1+BC and mass concentrations calculated by SMPS.

Table S1 Instruments used in the this study

Species	Instruments	Time resolution
NR-PM_1	HR-TOF-AMS	4 min
BC	Magee Scientific Aethalometer	2 min
Number size distribution	SMPS	10 min
SO_4^{2-}, NO_3^-, NH_4^+, Cl^-, Na^+ in $PM_{2.5}$	GAC-IC	30 min
VOCs	PTR-MS	30 s
VOCs	On-line GC/MS	1 h
CO	Enhanced Trace Level CO Analyzer	1 min
O_3	UV absorption ozone analyzer	1 min
Meteorology parameters	Automatic meteorological station	1 h

4 Excluding local influences

During the campaign, coal combustion and biomass burning plumes were observed. After field investigations, coal combustion was found to be from the mari-culture workshops, which burned coal to warm sea water for sea cucumbers. There are several mari-culture workshops located on the foot of the hill range, in the northeast direction of the Changdao site. When the wind came from northeast, “jump” concentration points from coal burning in AMS and other instruments were observed. Polycyclic aromatic hydrocarbon (PAHs) species are abundant in the emissions of domestic coal burning, which can account for 38% of organic aerosol mass from residential stove coal combustion (Zhang et al., 2008). To exclude local influence, naphthalene (m/z 129), a PAHs species measured by PTR-MS, was used to check coal combustion periods. By examining high concentrations (above 2 ng/m^3) and sharp peaks of naphthalene, 29 coal combustion events amounting to 40 hours in total were selected and shown in Fig.S2. Biomass burning influences from forest fires were also found during the campaign. Acetonitrile was usually regarded as an indicator for biomass burning emissions (de Gouw et al., 2003;Yuan et al., 2010). Two biomass burning events were masked by rapidly increased acetonitrile concentrations (yellow colored background), shown in the Fig. 2S. Detailed descriptions on the selection local influence data can be obtained from Yuan et al. (2012).

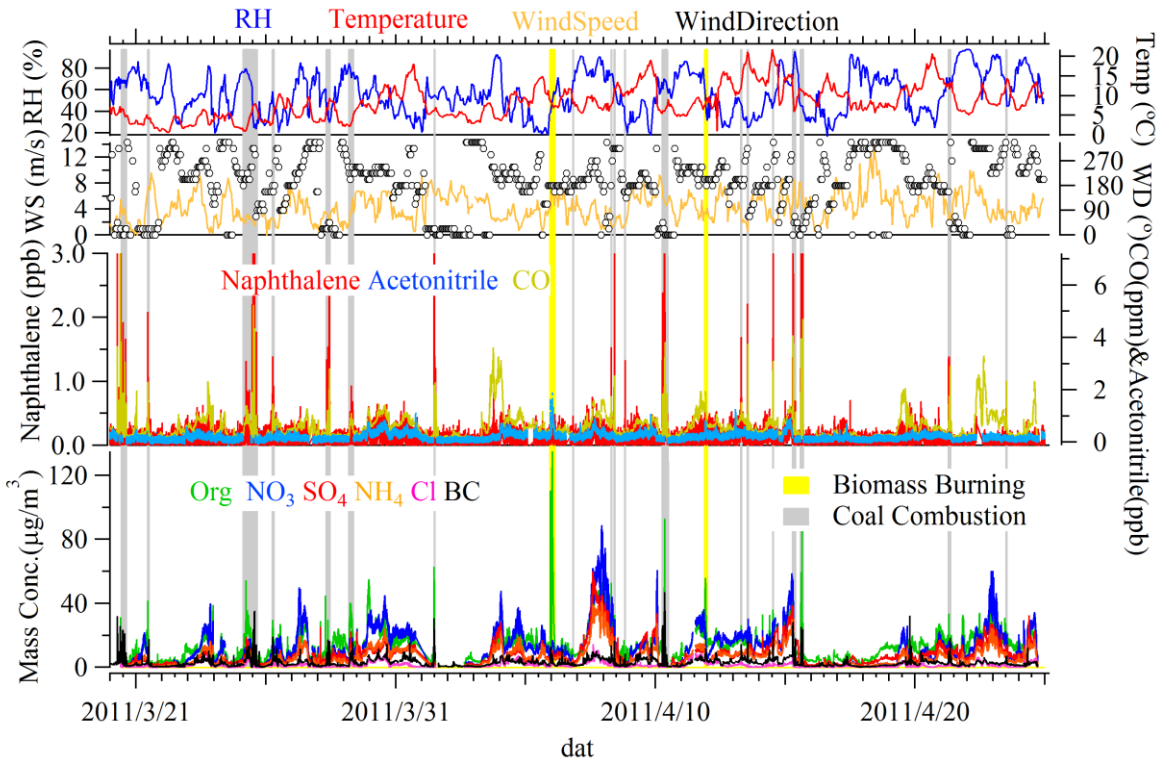

Figure S-6 Time series of meteorological parameters: relative humidity (RH), temperature (Temp); gases and VOCs: naphthalene, acetonitrile, CO; and AMS species+BC. The periods influenced by coal combustion were masked by gray color, and the biomass burning periods were masked by yellow color.

5 Comparison with AMS results from other sites

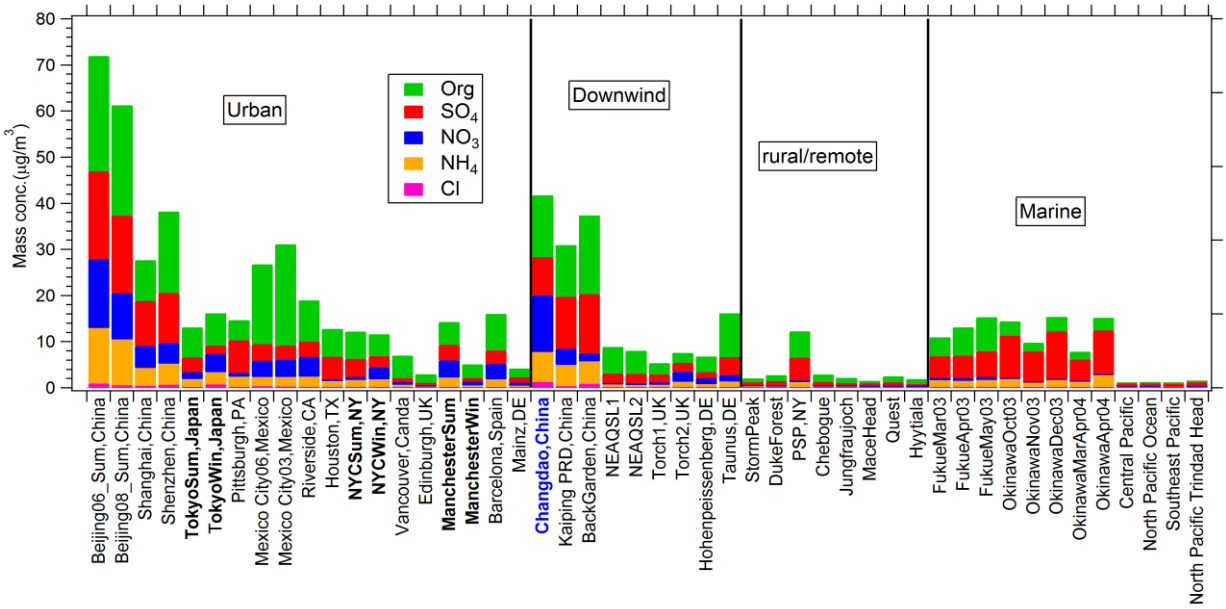

Figure S-7 Comparisons of PM_1 concentration and chemical composition with AMS results in other regions. The results were obtained from (Zhang et al., 2007;Huang et al., 2011;Huang et al., 2010;Huang et al., 2012;He et al., 2011;Xiao et al., 2011).

6 The determination of the PMF four-factor solution

The organic concentration influenced by local emissions usually increase rapidly and the corresponding data usually performs as “spikes”. The spike data points were found improper to be included in the PMF dataset, as they would increase the residual and make the results unstable(Ulbrich et al., 2009). Hence the data influenced by local coal burning and biomass burning are excluded in the PMF. Factor number from 1 to 10 as well as the different seeds (0-10) were selected to run in the model. A four-factor solution was selected for the final results. The performances of spectra and time series of the four factors at different Fpeak were also investigated. The detailed descriptions on the selection of PMF factor number and the performances of PMF factors on different solutions can be found in Table S2-3 and in Figure. S8-10.

Table S2 Descriptions of PMF solutions obtained at Changdao.

Factors	Fpeak	Seed	Q/Q_{exp}	Solution Description
1	0	0	4.41	Too few factors, large residuals at time series and key m/z
2	0	0	3.18	Too few factors, large residuals at time series and key m/z
3	0	0	2.86	Few factors (LV-OOA, SV-OOA, CCOA and HOA mixing). The Q/Q_{exp} at different seeds (0-10) are very unstable. Factors are mixing with each other.
4	0	**0**	**2.57**	**Optimum choices for PMF factors (LV-OOA, SV-OOA, HOA, CCOA). The time series and diurnal variations are consistent with the tracers. The spectra of the factors are corresponding to the source spectra in AMS spectra database.**
5	0	0	2.4	The time series of the extra factor can not be explained. The time serie of the fifth factors was noisy.
6-10	0	0	2.3-2.0	Slitting of factors happened, especially for the OOA factor. The noisy factor always existed.
4	-3.0-3.0	0	2.57-2.62	In FPEAK range from −1.0 to1.0, factor MS and time series are nearly identical, with variations less than 1%. For larger FPEAK, LV-OOA and SV-OOA became unstable.

4	0	0-250	2.57-5.18	Spectra and time series of each factors is stable.

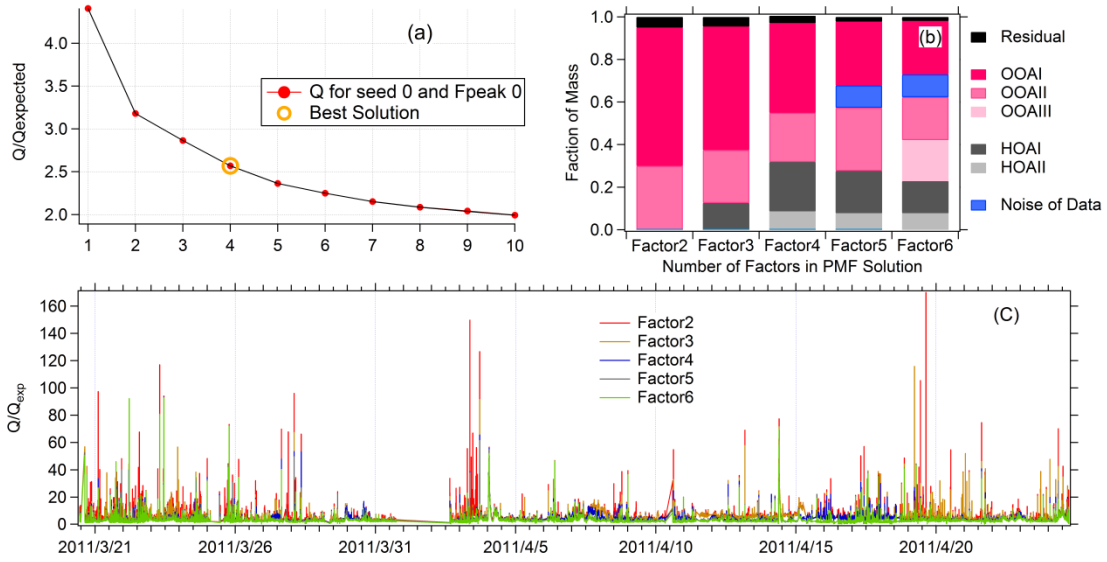

Figure S-8 The diagnostics plots of factor selections in PMF(Part I).

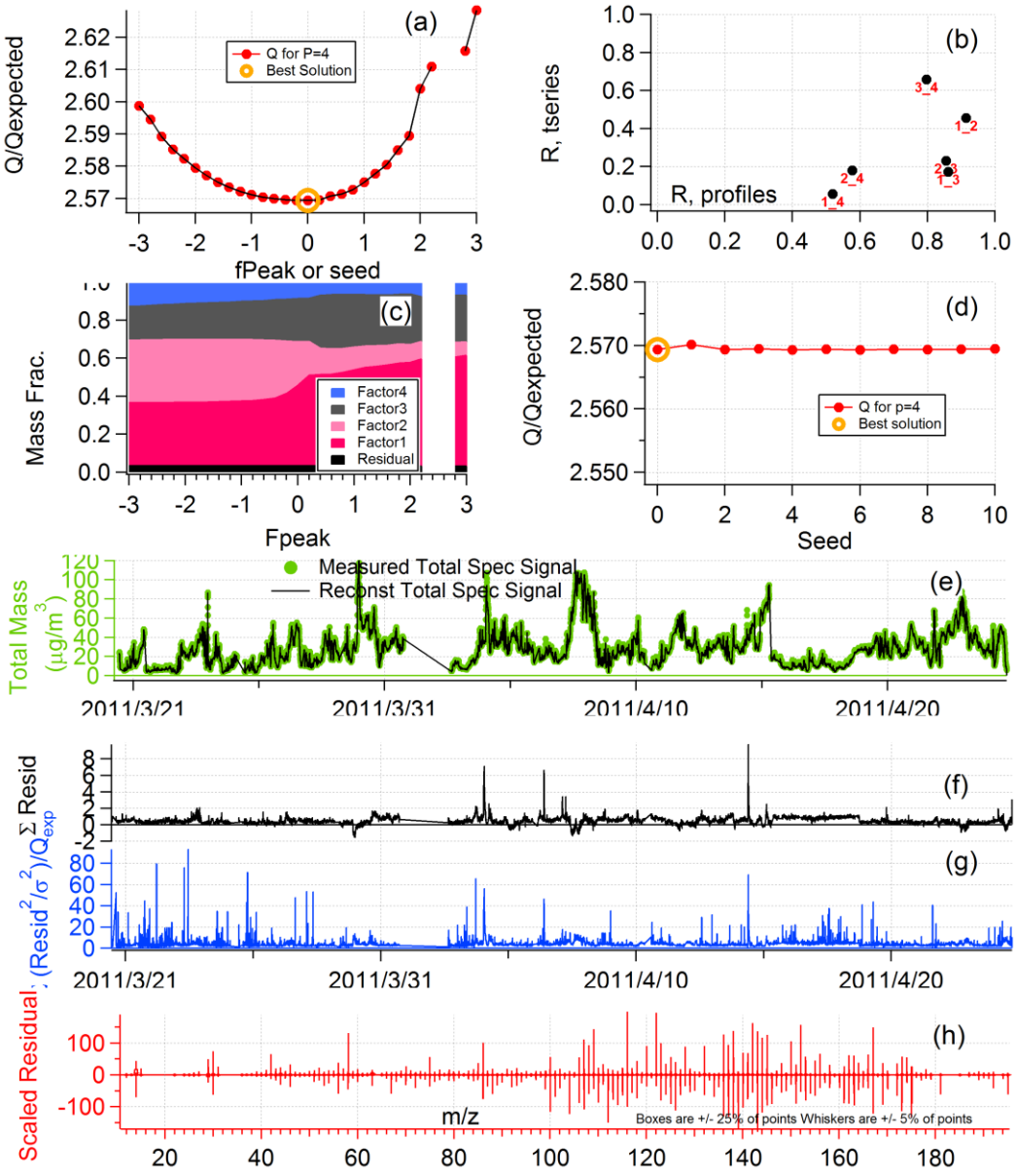

Figure S-9 The diagnostics plots of PMF selection (Part II).

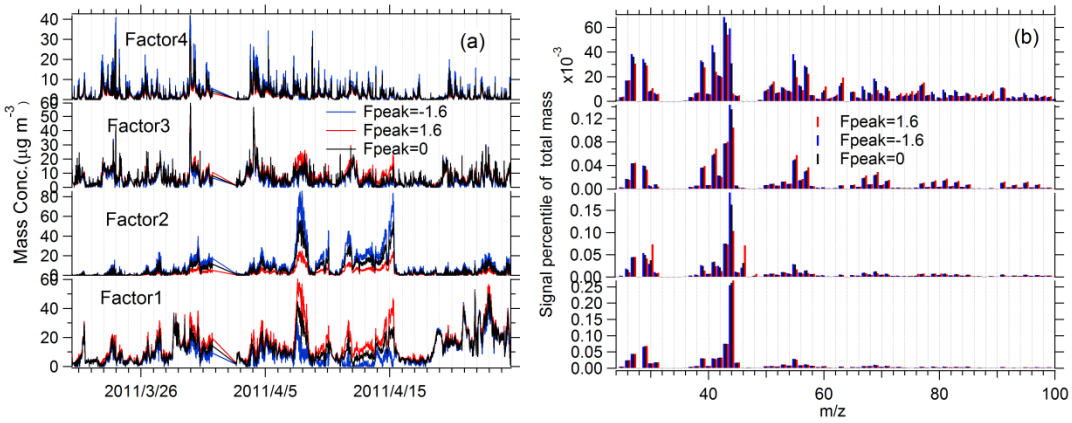

Figure S-10 The time series and spectra of 4-factors PMF solution at Fpeak=1.6,-1.6 and 0.

Table S3 The R between four factors with external species

	LV-OOA	SV-OOA	HOA	CCOA
SO_2	0.01	0.38	0.30	0.43
CO	0.33	0.44	0.60	0.44
NO	-0.02	-0.01	0.33	0.08
NO_x	0.17	0.41	0.69	0.42
NO_2	0.19	0.46	0.69	0.45
O_3	0.17	0.14	-0.41	-0.20
O_x	0.24	0.33	-0.09	0.02
SO_4	0.65	0.84	0.33	0.18
NO_3	0.62	0.85	0.48	0.31
NH_4	0.62	0.87	0.45	0.30
org	0.76	0.80	0.58	0.45
Cl^-	0.36	0.62	0.57	0.50
BC	0.37	0.69	0.53	0.57
Acetaldehyde	0.31	0.67	0.45	0.50
Toluene	0.19	0.52	0.62	0.60
Benzene	0.27	0.62	0.68	0.62
Acetone	0.37	0.66	0.23	0.33
Acetonitrile	0.29	0.61	0.43	0.54
Naphthalene	0.12	0.48	0.49	0.61

7 Back trajectory analysis

To explore the regional transport influences of Changdao site on PM_1 loading and compositions, a back trajectory analysis was performed by HYSPLIT 4.9 model (http://ready.arl.noaa.gov/HYSPLIT.php). The 48 hour back trajectories starting in Changdao were calculated every 2 hours during the entire campaign. All the back trajectories can be done clustering analysis due to their similarity in spatial distribution variations. The detailed description on how to do the cluster analysis and choose factors can be obtained on the user's manual for HYSPLIT model (Draxler, 2009). At last, 5 back trajectory clusters were achieved for the whole campaign as shown in Figure S-11. Clusters 1 to 5 accounted for about 7.1%, 35.9%, 24.1%, 23.2% and 9.7% of total clusters respectively.

The average PM_1 concentration and compositions were calculated according to cluster type, as shown in Fig.15. The most polluted cluster is from west of the Changdao site (cluster 2), the average PM_1 concentration can reach 60 μg m^{-3}. Then it is cluster 3 which is from the south direction and covers the area of Shandong Peninsula, the average PM_1 concentration is about 47.4 μg m^{-3}. The PM_1 mass concentrations corresponding to cluster1 is about 40.7 μg m^{-3}. Cluster 1 is from northwest and passes through the Beijing, Tianjin mega-city area. The cleaner plumes (cluster 4 and 5) originates from north part of China (Mongolia), where there is a lower population density than coastal area (Huang et al., 2010). The compositions of PM_1 shows distinct differences between pollutant plumes (cluster 1, 2, 3) and clean plumes (cluster 4, 5). The higher nitrate and chloride fraction of PM_1 in the pollutant plumes was found. However, for the clean plumes, organics and sulfate account for a higher mass percentage which is consistent with PM_1 composition reported in the clean area (Shank et al., 2012;Zhang et al., 2007). The relationship between organic compositions and clusters, as well as O/C and clusters, was also investigated here. The result showed that the clean plumes were dominated by the aged LV-OOA and showed higher O/C, indicating the high oxidation state of clean plumes. In contrast, the pollutant plumes were found with a higher POA (HOA+CCOA) and a lower O/C. The higher SV-OOA fraction was also found in the pollutant plumes, which is concrete with the conclusion that the SV-OOA was formed during the transportation.

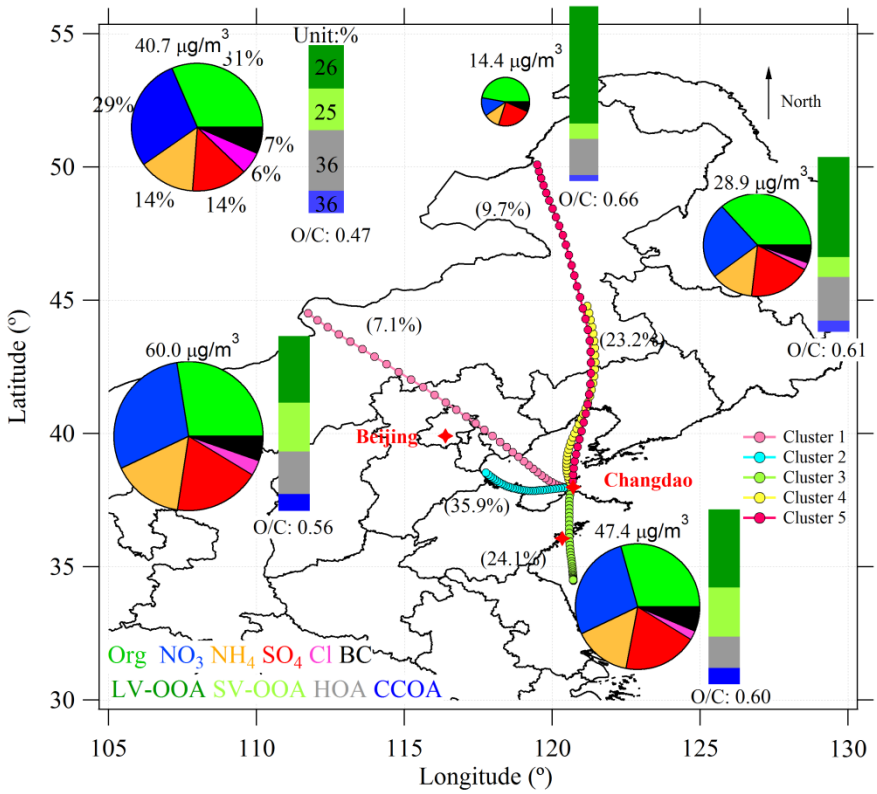

Figure S-11 The back trajectory clusters associated the corresponding average PM1 compositions, OA compositions and O/C.

8 A summary of k_{OH} values in the literatures

Table S4 The k_{OH} value of SOA reaction by different precursors The K_{OH} was calculated based on the assumption of average termperature of 8℃ at Changdao.

Reaction	k_{OH} ($\times 10^{-12}$ molecule^{-1} cm^3 s^{-1})	References
Biogenic reaction		
Isoporene	107	(Hodzic et al., 2009)
α-pinene	52.3	(Hodzic et al., 2009)
β-pinene	74.3	(Hodzic et al., 2009)
Anthropogenic reaction		
Toluene	5.63	(Hodzic et al., 2009)
m+p-xylene	18.9	(Hodzic et al., 2009)
Higher alkanes	2.3	(Hodzic et al., 2009)
anthropogenic VOCs	12.5	(Hodzic and Jimenez, 2011)
anthropogenic VOCs	5	(Spracklen et al., 2011)
Others		
POA aging to form SOA	3	(Hodzic and Jimenez, 2011)

References

de Gouw, J. A., et al.: Emission sources and ocean uptake of acetonitrile (CH3CN) in the atmosphere, J Geophys Res-Atmos, 108, Doi 10.1029/2002jd002897, Artn 4329

Doi 10.1029/2002jd002897, 2003.

Draxler, R., Stunder, B., Rolph, G.: HYSPLIT4 user's guide, Version 4.9, http://ready.arl.noaa.gov/HYSPLIT.php (last access: January 2010),, 2009.

He, L. Y., et al.: Submicron aerosol analysis and organic source apportionment in an urban atmosphere in Pearl River Delta of China using high-resolution aerosol mass spectrometry, J Geophys Res-Atmos, 116, 10.1029/2010JD014566, 10.1029/2010JD014566, 2011.

Hodzic, A., et al.: Modeling organic aerosols during MILAGRO: importance of biogenic secondary organic aerosols, Atmos Chem Phys, 9, 6949-6981, 2009.

Hodzic, A., and Jimenez, J. L.: Modeling anthropogenically controlled secondary organic aerosols in a megacity: a simplified framework for global and climate models, Geosci. Model Dev., 4, 901-917, 10.5194/gmd-4-901-2011<p>, 2011.

Huang, X. F., et al.: Highly time-resolved chemical characterization of atmospheric submicron particles during 2008 Beijing Olympic Games using an Aerodyne High-Resolution Aerosol Mass Spectrometer, Atmos Chem Phys, 10, 8933-8945, DOI 10.5194/acp-10-8933-2010, 2010.

Huang, X. F., et al.: Characterization of submicron aerosols at a rural site in Pearl River Delta of China using an Aerodyne High-Resolution Aerosol Mass Spectrometer, Atmos. Chem. Phys., 11, 1865-1877, 10.5194/acp-11-1865-2011, 2011.

Huang, X. F., et al.: Highly time-resolved chemical characterization of atmospheric fine particles during 2010 Shanghai World Expo, Atmos. Chem. Phys., 12, 4897-4907, 10.5194/acp-12-4897-2012, 2012.

Shank, L. M., et al.: Organic matter and non-refractory aerosol over the remote Southeast Pacific: oceanic and combustion sources, Atmos. Chem. Phys., 12, 557-576, 10.5194/acp-12-557-2012, 2012.

Spracklen, D. V., et al.: Aerosol mass spectrometer constraint on the global secondary organic aerosol budget, Atmos. Chem. Phys., 11, 12109-12136, 10.5194/acp-11-12109-2011, 2011.

Ulbrich, I. M., et al.: Interpretation of organic components from Positive Matrix Factorization of aerosol mass spectrometric data, Atmos Chem Phys, 9, 2891-2918, 2009.

Xiao, R., et al.: Characterization and source apportionment of submicron aerosol with aerosol mass spectrometer during the PRIDE-PRD 2006 campaign, Atmos. Chem. Phys., 11, 6911-6929, 10.5194/acp-11-6911-2011, 2011.

Yuan, B., et al.: Biomass Burning Contributions to Ambient VOCs Species at a Receptor Site in the Pearl River Delta (PRD), China, Environ Sci Technol, 44, 4577-4582, 10.1021/es1003389, 2010.

Yuan, B., et al.: VOCs emissions,evolution and its contribution to secondary organic aerosol (SOA) at a receptor site in eastern China, submitted to Atmos Chem Phys, 2012.

Zhang, Q., et al.: Ubiquity and dominance of oxygenated species in organic aerosols in anthropogenically-influenced Northern Hemisphere midlatitudes, Geophys Res Lett, 34, Doi 10.1029/2007gl029979, Artn L13801

Doi 10.1029/2007gl029979, 2007.

Zhang, Q., et al.: Asian emissions in 2006 for the NASA INTEX-B mission, Atmos Chem Phys, 9, 5131-5153, 2009.

Zhang, Y. X., et al.: Characteristics of particulate carbon emissions from real-world Chinese coal combustion, Environ Sci Technol, 42, 5068-5073, Doi 10.1021/Es7022576, 2008.